Supporting Material

Markus Düttmann* [1], Yuichi Togashi[2,3,4], Toshio Yanagida[4,5], Alexander S. Mikhailov[1]

[1]Department of Physical Chemistry, Fritz Haber Institute of the Max Planck Society, Berlin, Germany
[2]Department of Computational Science, Graduate School of System Informatics,Kobe University, Hyogo, Japan
[3]Applied Information Systems Division, Cybermedia Center, Osaka University, Osaka, Japan
[4]Quantitative Biology Center, RIKEN, Osaka , Japan
[5]Soft Biosystem Group, Graduate School of Frontier Biosciences, Osaka University, Osaka, Japan

*Corresponding author. Address: Department of Physical Chemistry, Fritz Haber Institute of the Max Planck Society, Faradayweg 4-6, 14195 Berlin, Germany, Tel.: +49 30 8413 5301, Email: duettmann@fhi-berlin.mpg.de

Immobilization procedure

If a force acts on a single node of an elastic network, it induces not only internal deformations in the network, but also rigid translations and rotations of the entire object. If the network is pinned, e.g. by immobilizing one of its nodes, this can introduce additional internal deformations and the results of the study would depend on the location of the pinned node. To avoid such effects in our simulation, we have employed a special immobilization procedure. Compensating forces were applied to all network nodes in such a way that they could only lead themselves to a rigid translation or rotation. The magnitudes of the additional forces were determined by the condition that prevented translational and rotational motions induced by the external force. The computation of compensating forces was performed at each next integration step, so that they were automatically adjusted to the conformational changes.

To construct compensating forces, we first note that, if the same force $\mathbf{f}$ is applied to each particle, it would lead to a rigid translation of the entire network. Moreover, if forces $\mathbf{f}_i = \boldsymbol{\omega} \times \mathbf{R}_i$ with an arbitrary vector $\boldsymbol{\omega}$ are applied to the particles with coordinates $\mathbf{R}_i$, they can induce only rigid rotation.

Without loss of generality, the coordinates $\mathbf{R}_i$ can always be chosen in the coordinate frame whose origin coincides with the center of mass of the network. Suppose that an external force $\mathbf{F}_{\text{ext}}$ acts on a particle with coordinates $\mathbf{R}_0$. Then, it generates an external torque $\mathbf{R}_0 \times \mathbf{F}_{\text{ext}}$ that should be balanced by some compensating forces $\mathbf{f}_i$. These additional forces should therefore satisfy the balance equation

$$\mathbf{R}_0 \times \mathbf{F}_{\text{ext}} + \sum_{i=1}^{N} \mathbf{R}_i \times \mathbf{f}_i = 0\,, \tag{S1}$$

which can be rewritten as

$$-\mathbf{M}\boldsymbol{\omega} = \mathbf{R}_0 \times \mathbf{F}_{\text{ext}} \tag{S2}$$

with the matrix

$$\mathbf{M} = \sum_{i=1}^{N} \begin{pmatrix} |\mathbf{R}_i|^2 - X_i^2 & -X_i Y_i & -X_i Z_i \\ -X_i Y_i & |\mathbf{R}_i|^2 - Y_i^2 & -Y_i Z_i \\ -X_i Z_i & -Y_i Z_i & |\mathbf{R}_i|^2 - Z_i^2 \end{pmatrix}. \tag{S3}$$

Thus, to prevent rigid rotation, additional forces

$$\mathbf{f}_i = -\left[\mathbf{M}^{-1}\left(\mathbf{R}_0 \times \mathbf{F}_{\text{ext}}\right)\right] \times \mathbf{R}_i \tag{S4}$$

should be supplied. Note that, as can be easily checked, $\sum_i \mathbf{f}_i = 0$ and, hence, such compensating forces do not induce translational motion of the network. To prevent rigid translation induced by the external force, the compensating force $\mathbf{f} = -\mathbf{F}_{\text{ext}}/N$ should be additionally applied to each network node.

Thus, if compensating forces $\mathbf{f} + \mathbf{f}_i$ are applied to all nodes at every integration step, both translation and rotation induced by the external force can be balanced out in a noninvasive manner.

Myosin Directions

Myosin-V walks along the filament in the direction of the barbed end. In the experiments, the protein was dragged along the filament. The forward strain direction corresponded to the direction of processive motion, whereas the backward direction was opposite to it. If one wants to computationally reproduce the experimental situation, forward and backward directions for the elastic network of the protein must be identified. We have done this by including F-actin into the elastic network simulations and determining the equilibrium conformation of the myosin-actin complex.

Employing guided MD simulations, Lorenz and Holmes (1, 2) have recently identified several possible binding sites of myosin-II to actin. Comparing structures of myosin-II and myosin-V, analogous binding sites for myosin-V can be suggested. The myosin head binds to two distinct F-actin monomers in the filament (constructed from PDB ID: 2ZWH (3)) at the positions given in Table S1.

To determine the equilibrium position of myosin with respect to the actin filament, the following procedure has been employed: Elastic links, connecting myosin to the actin filament, have been introduced with equilibrium lengths of 3.5 Å and stiffness $\kappa = 1$. After that, relaxation equations (3) of the myosin-actin complex were numerically integrated until a stationary state has been reached. In this way, we approximated the actomyosin

Table S1: Links between myosin and actin monomers in the filament

myosin	1st actin monomer	2nd actin monomer
343	328	-
386	337	-
517	167	-
526	-	50
542	-	95

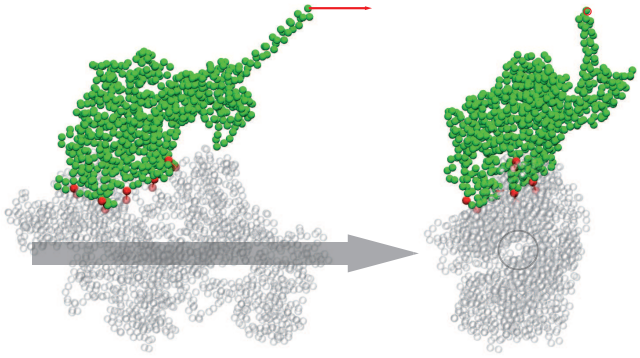

Figure S1: Myosin-V modeled on actin filament: the elastic network (green) is anchored to the actin at specific binding sites (red balls mark corresponding residues on myosin and actin, respectively). The direction of the processive motion is shown by the gray arrow and the force applied by the red arrow.

structure as shown in Fig. S1.

Relaxation to the equilibrium state of the complex involved rotation of the myosin-V molecule, To quantify this rotation, we have chosen four residues (165, 195, 559, 691). These residues belong to the stiff core of the protein. With these residues, one can construct three linear independent vectors that define a coordinate system only in terms of the network structure. Thus, the forward direction $\mathbf{n}_{\|}$ can be approximated by transforming the filament axis to the coordinate frame of the reference state (PDB ID: 1W7J) (4) that is defined by the same residues. In this way, we found the forward direction to be approximately $\mathbf{n}_{\|} = (-0.254, -0.888, 0.383)$.

Sensitivity Tables

Our aim is to examine the mechanical responses of the protein to forces with varying directions applied to individual residues in the nucleotide-binding pocket and actin-binding cleft. To probe mechanical responses, we select two sets of residues in the respective regions (see Fig. 2a). For every chosen residue, a series of 200 simulations was performed. In all simulations, the magnitude of the applied force was the same ($f_0 = 1$ Å), but its orientations were randomly varied. The simulations were continued until a stationary state was found. After that, changes in the monitored pair distances between the labels in different regions were determined. The induced distance changes were analyzed and, for each pair of labels, the maximum absolute distance change of 200 force orientations was evaluated. In this way, we obtained the sensitivity to forces applied to a residue with respect to a particular pair distance.

The results are shown in Tables S2 and S3 and will be commented below. Note that absolute sensitivities for different pairs of labels cannot be compared. As a matter of fact, distance changes for the tail are always larger than for the actin-binding cleft. To show the variations of sensitivity, a color code was employed. In each column, the maximum and the minimum entries are taken and color gradations from dark blue for the minimum to dark red for the maximum are applied.

Forces in the nucleotide-binding region

In the NBP, a set of 27 residues adjacent to the ATP in the considered equilibrium conformation was selected (left column Table S2 and Fig. 2a). The sensitivities of these residues with respect to different pair distances are shown in Table S2. The left column lists the residues and, in each of the other columns, the sensitivities with respect to the distance between a particular pair of labels (e.g., between residues 343 and 517) are given.

The last two columns of Table S2 show the sensitivity of the tail with respect to forces in the NBP. Applying forces to the residues 115 and 116 or their neighbors, a strong effect on the tail is induced. These two residues are located in the front-door region (Fig. 4). Remarkably, applying forces to residues in the back door (219, 220 and 438–442) or the P-loop (163–169) only weakly affects the tail region. Thus, the tail responds mainly to the perturbations applied at the entrance of the front door.

Moreover, sensitivity with respect to residues in the actin-binding cleft was investigated. The strongest response with respect to the distance 343-

517 characterizing cleft opening is seen if forces are applied to the residue 442, which belongs to the back-door region. Additionally, perturbations near the front-door residues 115 and 116 show some effect. The distance between residues 386 and 517 describes cleft opening, but mostly reflects movement of the HCM loop to which residue 386 belongs. Here, large responses were observed when the forces were applied in the back-door region with the strongest sensitivity to the perturbations of residues 219 and 220. Only small changes were seen if the forces were applied in the front-door area.

In terms of the sensitivity of its residues, the NBP region is clearly divided into a front-door and a back-door domain (Fig. 4). A pronounced effect on the actin cleft was observed when forces were applied to residues 219, 220 and 442 in the back-door region. Remarkably, it is exactly the salt bridge between residues 219 and 442 that hinders phosphate release after the hydrolysis. The P-loop region is seen to be relatively stiff and external forces here do not induce large conformational changes in the tail or the actin cleft. Perturbations in the front door affect the tail.

Forces in the actin-cleft region

Using the results of Lorenz and Holmes (1, 2), we identified 54 residues which may come in contact with the filament (left column Table S3 and Fig. 2a). To study communication between the actin-binding region and the NBP or the tail, we repeat the simulation procedure described above and obtain the sensitivities shown in Table S3.

As can be seen from the results, application of forces to the HCM loop (residues 377 to 390) can induce strong responses of the tail. Moreover, there is some effect on the distance between residues 789 and 92 in the tail region to the forces applied at the residues from 340 to 350, which belong to the upper 50kDa subdomain, as well. Remarkably, the tail is only weakly affected by the forces applied to the residues in the lower 50kDa subdomain.

The front door (distance between residues 115 and 297) is strongly sensitive to the forces applied at the upper 50kDa subdomain, including the HCM loop. The back door (distance between residues 442 and 291) is mostly sensitive to the forces applied to residues 540 to 544 in the lower 50kDa subdomain; it should however be noted that these residues are located near the back door and, therefore, stronger sensitivity might have been expected.

Comparison to the linearized model

The relaxation equations (3) of the elastic network are linear in terms of the distance changes between the particles. They are, however, still nonlinear in terms of the changes of the absolute coordinates of the particles $\mathbf{r}_i = \mathbf{R}_i - \mathbf{R}_i^{(0)}$, since the distance d_{ij} is a nonlinear function of the coordinates $\mathbf{R}_i$ and $\mathbf{R}_j$. Note that not the distance, but the particle coordinates are the dynamical variables in these equations. Hence, to proceed further to the linear (or harmonic) approximation, equations (3) need to be linearized with respect to the coordinate changes $\mathbf{r}_i$. After linearization, they take the form

$$\dot{\mathbf{r}}_i = \mathbf{F}_i - \sum_{j=1}^{N} \mathrm{A}_{ij} \frac{\mathbf{R}_i^{(0)} - \mathbf{R}_j^{(0)}}{\left(d_{ij}^{(0)}\right)^2} \left[\left(\mathbf{R}_i^{(0)} - \mathbf{R}_j^{(0)} \right) \cdot (\mathbf{r}_i - \mathbf{r}_j) \right] . \qquad \text{(S5)}$$

This system of linear equations can further be used to obtain the eigenvalues and the eigenvectors corresponding to various normal modes. It should be noted that, although the overdamped limit of relaxational dynamics is considered here, the resulting eigenvalues and eigenvectors are still the same as when the purely inertial (vibrational) dynamics is assumed.

The linearized equations (S5) can be used as long as all coordinate changes $\mathbf{r}_i$ are much smaller than the (natural) lengths of the elastic links connecting neighbor particles. Therefore, to test the possible validity of the linear approximation, the observed coordinate changes should be compared with the typical natural lengths of the elastic links. By the construction of the EN model, natural lengths of all elastic links cannot exceed the cutoff length, which has been 10Å in the present study. The average natural length l_{av} of a link is smaller and, for a rough estimate, the value $l_{\mathrm{av}} = 5$Å can be chosen. Linearization holds if the coordinate changes $\mathbf{r}_i$ are much smaller than l_{av}, which requires that they should not exceed, e.g., 10% of l_{av}, that is they cannot be larger than 0.5Å.

When the effects of forward strain were considered, an external force with the magnitude $f = 6$Å was applied to the tail and, after a new equilibrium state was reached, conformational changes have been inspected and changes of the distances between the labels were analyzed. We have also checked what were the deviations in the absolute positions of some typical residues. As it turns out, when such a force is applied to the tail, the position of the characteristic residue 384 in the HCM loop gets changed by $r_{384} =$ 7.4Å. Moreover, the residue 792, which is located in the tail, moves by 12.2Å from its equilibrium position. Such displacements are comparable

to the cutoff length and, thus, when responses in the actin cleft or in the tail are considered, the linear description cannot hold. On the other hand, the respective induced changes within the nucleotide binding pocket are much smaller. For example, residue 115 in the front door region shifts its position by only $r_{115} = 0.6$Å when the same force is applied to the tail. Such weaker changes in the nucleotide-binding region could probably have also been correctly reproduced within the local linear approximation for this protein region.

The limitations of the linearized normal-mode descriptions have been previously discussed for myosin-V and kinesin (6). In the present study, we have decided to stay completely within the full nonlinear elastic description, so that such difficulties cannot arise. Because the linearized equations are only an approximation to the full set of nonlinear equations, considered here, their analysis, once performed within the validity region of the approximation, cannot obviously yield anything which is not already contained in the nonlinear model.

As an illustration of the difficulties encountered in the linearized description, Fig. S2 shows the behavior described by the linearized equations (S5) as compared with the responses described by the full nonlinear equations (3). Here, a constant force $\mathbf{f} = (-1, 1, 1)/\sqrt{3}$ Å is applied to residue 384 in the HCM loop. The dynamical responses of the elastic network are determined by integration of equations (3) or (S5), respectively. The absolute displacements r_{115} and r_{792} of the residues 115 and 792, located in the front-door region and the tail, respectively, are plotted here as functions of time for both descriptions. As we see, the full nonlinear equations yield the responses (solid curves) which saturate as the new equilibrium state of the network, under the constant applied force, is approached. In contrast to this expected behavior, integration of the linearized equations yields the displacements which indefinitely grow with time (dashed curves in Fig. S2).

Such unphysical behavior has been observed because the linearized equations have been used in the above example beyond their validity limit. Indeed, the final stationary displacements of the considered residues in the full nonlinear model are of the order of tens of Å in this case, strongly exceeding what is required for the validity of the linearized description. The origin of the observed unphysical divergence lies in the fact that, after linearization, the energy of an elastic network does not depend on the displacement components of particles which are orthogonal to the directions of equilibrium links between them (cf. equations (S5)). Therefore, such displacements may indeed grow indefinitely without increasing the energy of the linearized system. In the full nonlinear model, the energy is invariant, on the other

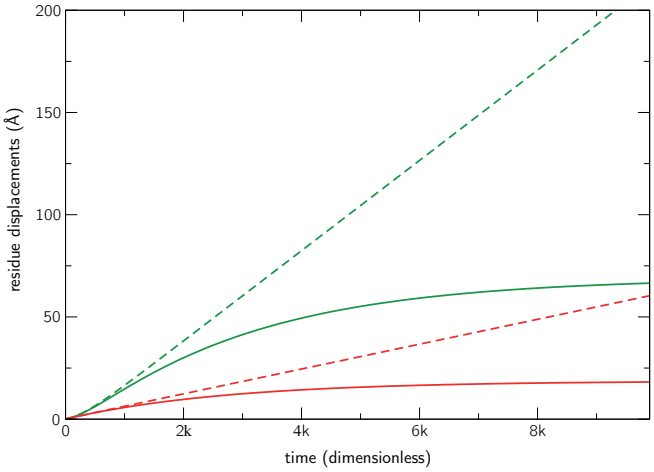

Figure S2: Comparison of the network responses to the application of a static force to the tail, as yielded by the full nonlinear and the linearized models. Constant force of amplitude $f = 0.5$Å and direction $(-1, 1, 1)/\sqrt{3}$ is applied to residue 384 in the HCM loop. Time-dependent displacements r_{792} (green) and r_{115} (red) of residues 792 and 115 from their equilibrium positions are displayed, as yielded by the integration of the full nonlinear (3) (solid curves) and the linearized equations of motion (S5) (dashed curves) can be compared.

hand, only under the displacements of particles which preserve distances between all of them, i.e the lengths of all elastic links. They correspond to rigid translations and rotations of the entire network, always eliminated in our simulations via the immobilization procedure.

References

1. Holmes K. C., R. R. Schröder, H. L. Sweeney, and A. Houdusse. 2004. The structure of the rigor complex and its implications for the power stroke. *Phil. Trans. R. Soc. B.* 359:1819–1828.

2. Lorenz M., and K. C. Holmes. 2010. The actin-myosin interface. *Proc.*

Natl. Acad. Sci. USA. 107:12529–12534.

3. Oda T., M. Iwasa, T. Aihara, Y. Maeda, and A. Narita. 2009. The nature of the globular- to fibrous-actin transition. *Nature.* 457:441–445.

4. Coureux P. D., H. L. Sweeney, and A. Houdusse. 2004. Three myosin V structures delineate essential features of chemo-mechanical transduction. *Embo J.* 23:4527–4537.

5. Atilgan C, and A. R. Atilgan. 2009. Perturbation-Response Scanning Reveals Ligand Entry-Exit Mechanisms of Ferric Binding Protein. *PLoS Comp. Biol.* 5:e1000544.

6. Togashi Y., T. Yanagida, and A. S. Mikhailov. 2010. Nonlinearity of mechanochemical motions in motor proteins. *PLoS Comput. Biol.* 6:e1000814.

Table S2: Maximal distance changes (Å) observed when forces are applied to different residues in the nucleotide-binding pocket

residue	343 to 517	386 to 517	789 to 141	789 to 92
111	0.126	0.069	7.199	6.346
112	0.134	0.078	8.275	7.231
113	0.148	0.067	8.029	7.222
114	0.146	0.104	9.112	8.065
115	0.171	0.140	9.517	8.533
116	0.167	0.138	9.825	8.476
163	0.124	0.167	4.304	3.719
164	0.137	0.186	4.131	3.746
165	0.140	0.203	4.001	3.869
166	0.131	0.157	4.897	4.817
167	0.123	0.126	5.439	4.827
168	0.121	0.117	5.768	5.114
169	0.114	0.156	4.859	4.279
170	0.107	0.188	5.171	4.494
171	0.109	0.148	6.395	5.468
214	0.075	0.244	4.953	5.040
215	0.048	0.305	5.523	5.615
216	0.066	0.282	5.362	5.299
217	0.068	0.292	4.168	4.303
218	0.090	0.307	3.580	3.669
219	0.087	0.336	2.644	2.983
220	0.125	0.333	2.310	2.359
438	0.106	0.255	2.364	2.159
439	0.135	0.250	2.274	2.203
440	0.134	0.229	2.852	2.722
441	0.144	0.272	3.004	2.682
442	0.228	0.286	2.956	2.470

Table S3: Maximal distance changes (Å) observed when forces are applied to different residues in the actin-binding pocket

residue	789 to 141	789 to 92	115 to 297	442 to 219
340	4.911	6.086	0.359	0.095
341	5.103	6.191	0.409	0.107
342	5.431	5.790	0.430	0.111
343	6.643	6.378	0.466	0.107
344	6.884	6.007	0.480	0.118
345	6.531	5.374	0.468	0.127
346	6.919	5.619	0.442	0.111
347	6.898	6.160	0.423	0.094
348	6.226	6.104	0.401	0.090
349	6.545	6.892	0.388	0.079
350	6.376	7.288	0.357	0.077
377	7.457	6.754	0.341	0.061
378	7.395	6.492	0.332	0.069
379	8.492	7.168	0.346	0.075
380	9.036	7.613	0.370	0.098
381	9.204	7.994	0.385	0.109
382	9.377	7.998	0.395	0.106
383	9.533	8.123	0.403	0.116
384	9.374	8.130	0.411	0.107
385	9.494	8.152	0.420	0.102
386	9.359	8.028	0.412	0.103
387	9.425	8.161	0.418	0.101
388	9.163	7.815	0.399	0.071
389	8.631	7.215	0.410	0.081
390	7.634	6.752	0.397	0.078
500	3.929	3.617	0.136	0.019
501	4.952	4.752	0.155	0.053
502	5.688	5.403	0.184	0.069
503	5.905	5.307	0.199	0.055
504	5.216	4.540	0.177	0.035
505	4.631	3.732	0.163	0.021
506	4.074	3.315	0.140	0.020
516	6.723	5.423	0.207	0.103
517	6.591	5.050	0.179	0.080
518	6.065	4.319	0.171	0.058
519	5.378	3.560	0.162	0.067
520	4.713	2.870	0.163	0.075
521	5.584	3.334	0.202	0.072
522	6.114	4.012	0.207	0.038
523	5.386	3.621	0.191	0.033
524	5.261	3.627	0.208	0.064
525	6.319	4.426	0.236	0.060
526	6.227	4.830	0.228	0.037
527	5.616	4.385	0.218	0.056
528	6.419	5.106	0.252	0.089
529	6.908	5.667	0.272	0.088
530	6.689	5.728	0.249	0.086
540	6.058	4.730	0.260	0.145
541	5.986	4.442	0.267	0.172
542	6.953	4.672	0.292	0.199
543	7.004	4.175	0.287	0.197
544	5.939	3.638	0.262	0.160
545	5.990	3.735	0.253	0.125
634	4.464	3.959	0.100	0.117

Movie S1: A constant force with amplitude $f = 6$Å in the forward direction $(-0.254, -0.888, 0.383)$ is applied to residue 792 in the tail region and the equations of motion (3) are integrated. The movie shows relaxation to the new stationary conformation, starting from the equilibrium conformation of the network. The force is indicated by a red arrow.

Movie S2: A constant force $(-1, 0, 0)$ Å is applied to residue 115 in the front-door region and the equations of motion (3) are integrated. This movie shows the relaxation to the new stationary conformation, starting from the equilibrium conformation. The force is indicated by the a arrow.

Movie S3: A constant force $(-1, 1, 1)/\sqrt{3}$ Å is applied to residue 384 in the HCM loop and the equations of motion (3) are integrated. This movie shows the relaxation to the new stationary conformation, starting from the equilibrium conformation. The force is indicated by a red arrow.